# Performance Characterization of Computed Radiography based Mammography Systems

Abhinav Singh[a,c] , Nikunj Desai[a,c] and Daniel J Valentino[a,b]

[a]*i*CR Company Inc, 2580 West 237th Street, Torrance, CA 90505, USA;
[b]Department of Radiology, University of California, LA, CA 90024, USA;
[c]Department of Biomedical Engineering, University of California, LA, CA 90024, USA

## ABSTRACT

Computed Radiography (CR) is a cost-effective technology for digital mammography. In order to optimize the quality of images obtained using CR Mammography, we characterized the effect on image quality of the electro-optical components of the CR imaging chain. The metrics used to assess the image quality included the Contrast to Noise Ratio (CNR), Modulation Transfer Function (MTF), Noise Power Spectrum (NPS), Detective Quantum Efficiency (DQE) and Contrast Detail Response Phantom (CDMAM 3.4 Artinis Medical Systems). An 18x24 cm high-resolution granular phosphor imaging plate (AGFA MM3.0) was used to acquire the images. Contrast detail was measured using a GUI developed for the CDMAM phantom that was scored by independent observers. The range of theoretically acceptable values measured for the CR laser was (5-36) mW and voltage range for PMT's was (4-8) V. The light detection amplifier was investigated, and the optimal Laser Power and PMT gain used for scanning was measured. The tools that we used (CNR, MTF, NPS, DQE and Contrast-detail phantom) provided an effective means of selecting optimal values for the electro-optical components of the system. The procedure enabled us to obtain good quality CR mammograms that have less noise and improved contrast.

**Keywords:** Computed Radiography, Mammography, Modulation Transfer Function, Noise Power Spectrum, Detective Quantum Efficiency, Photomultiplier tube, CDMAM 3.4 Phantom

## 1. INTRODUCTION

Mammography is the most widely accepted procedure for the early detection of breast cancer. It is also one of the most demanding radiological examinations both diagnostically and technically because the background morphology of the breast can range from very low contrast areas to very high contrast areas and it is essential that objects with very small contrast and diameter can be distinguished.[1] There is a requirement of optimum contrast and low noise in mammograms for the detection of ductal and invasive carcinomas and to distinguish cancer from other benign lesions in the breast.[2] Computed Radiography (CR) is a cost-effective technology for digital mammography. There has been previous reports on performance characterization of a dual-side read and a single-side read dedicated mammography computed radiography system.[3] In computed radiography, the imaging plate and x-ray tube are two of the major factors that determine the quality of the image obtained, while the lasers used to scan the phosphor imaging plate and the photomultiplier tube gain are two of the variable components that can be adjusted to optimize the quality of the image obtained. We can optimize the quality of the CR based Mammography system by selecting the optimal values for the electro-optical components. For evaluation of the image quality, we can plot the Contrast to Noise Ratio (CNR), Modulation Transfer Function (MTF), Noise Power Spectrum (NPS) and Detective Quantum Efficiency (DQE) and the Contrast-detail curves using the CDMAM Phantom. These physics tools characterize the contrast transfer properties, noise properties and overall x-ray utilization efficiency of the system, respectively.[3] Varying the values of the Laser Power and Photomultiplier Tube (PMT) of the system yields different results. Hence, we can vary these electro-optical parameters (Laser Voltage and PMT Voltage) until we obtain optimal values for the system.

E-mail:asingh@icrcompany.com, dvalentino@icrcompany.com, Website: www.icrcompany.com

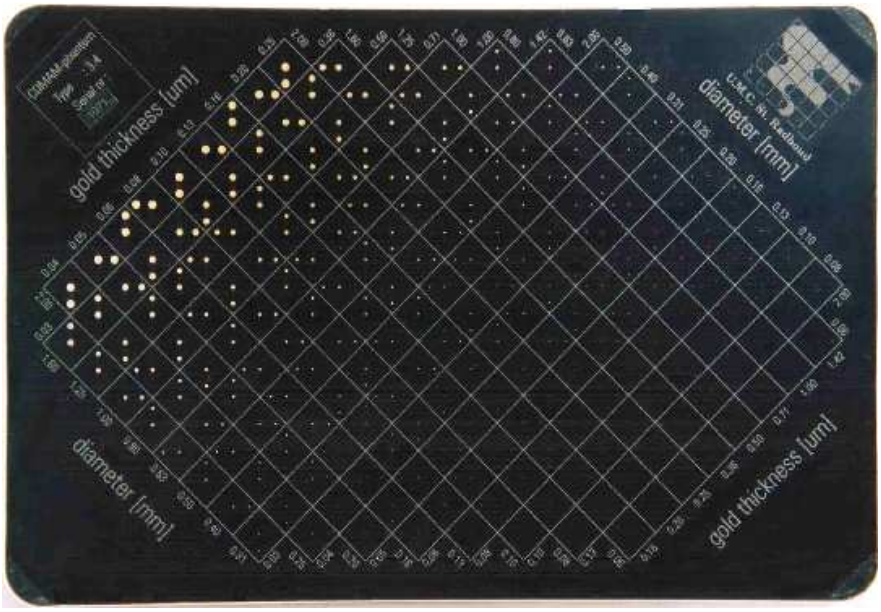


Figure 1. Image of a CDMAM 3.4 Phantom from Artinis Medical Systems, Netherlands.

## 2. MATERIALS AND METHODS

### 2.1 Imaging Systems and X-Ray Beam Properties

In this study, the beam quality specified in IEC 62220-1-2 for mammography was followed. To obtain the Modulation Transfer Function, Noise Power Spectrum and Detective Quantum Efficiency, a tube voltage of 28 Kv was used, with 2mm of added aluminum filtration placed close to the x-ray tube.[4] The Aluminum filter at the output of the tube was sufficient to reproduce the soft x-ray scatter conditions found at the output of an anti-scatter grid used in clinical conditions. The exposures were taken on a LORAD M-III Mammography X-ray system and all the images were acquired using a large (0.3mm) focal spot. The X-Ray tube has a molybdenum (Mo) filter and a rhodium (Rh) filter.[3] AGFA's MM 3.0 (High-resolution phosphor imaging plate) was used as the detector. The high-resolution imaging plates were scanned in computed radiography-based mammography system(iCRco 3600M, iCRco. Inc, Torrance, CA). The photostimulable phosphor (PSP) imaging plate is comprised of an unstructured layer of europium activated barium fluorobromide (BaFBr:Eu).[5] The imaging plates were erased before the beginning of the measurements and images were obtained by placing the CR cassettes on top of the bucky. The laser used for the study is a solid-state diode (wavelength=658 nm). The solid-state diode lasers are more compact, energy-efficiect and have a longer operational lifetime than gas lasers.[6] A dosimeter was used to measure the dose at the surface of detectors. The tube current-exposure time product was varied to give different values of air kerma at the detector entrance surface.

### 2.2 CDMAM 3.4 Contrast Detail Phantom

The Artinis CDMAM 3.4 Phantom (version 3.4, Artinis, St. Walburg 4, 6671 AS Zetten, The Netherlands) was used to characterize the ability of the system to detect very low contrast and very small details. The CDMAM Phantom consists of an aluminum base with gold discs of various thickness and diameter. The aluminum base is attached to a plexiglas (PMMA) cover. Contrast detail measurements rely upon a large number of observer readings. This procedure has two drawbacks. One is the large amount of time consumed using human observers and the other is the presence of significant inter-observer error when performed by different human observers.[1] To overcome this, there is a basic software tool described by Karssemeijer and Thijssen[7] that automatically identifies discs on digital images of the CDMAM. The software tool is called CDCOM and is available via the EUREF website.[8]

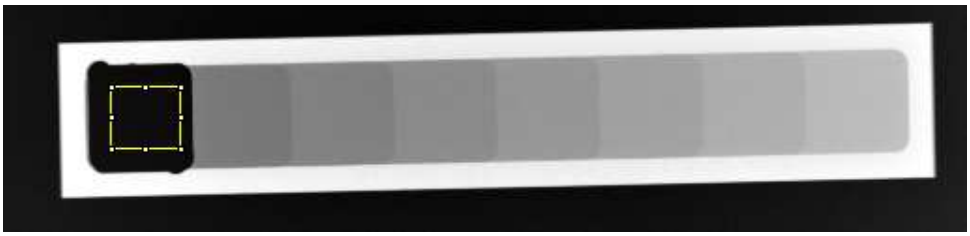

Figure 2. The CNR step-wedge phantom and the ROI created by the software as it appears on the image.

It is also known that contrast resolution in terms of threshold contrast visibility rather than spatial resolution is the best metric for characterizing and comparing the imaging performance of mammographic systems.[9]

### 2.3 Contrast to Noise Ratio (CNR)

Contrast and noise are two basic metrics of image quality. In this study, the CNR was used to differentiate between images obtained by altering the settings for laser power and the PMT Gain. CNR is defined as the ratio of difference of signal intensities of two regions of interest to the background noise. To measure Contrast to Noise Ratio, we used an Aluminum step-wedge phantom to simulate the approximate anatomical attenuation. There is a step increment of seven different thicknesses that simulates fine subject contrast. Figure 2 illustrates the manner in which the CNR step-wedge phantom appears on the scanned CR image. The ROI (Region of Interest) created on this image needs to be moved across the step-wedge by the user. This helps to obtain the statistics of all the steps of this step-wedge.[10] Acrylic sheets of varying thickness were used to simulate the tissue scatter observed in anatomical images from patients or phantoms. The step-wedge was sandwiched between these acrylic sheets and the entire setup was exposed at an appropriate dose.

The contrast to noise ratio was measured using Equation 1:

$$CNR = \frac{(S_a - S_b)}{N_{bg}}, \tag{1}$$

where $S_a$ is the signal intensity of region a, $S_b$ is the signal intensity of region b and $N_bg$ is the background noise.

### 2.4 Modulation transfer function(MTF)

The MTF is a basic performance measure of an imaging system that describes the signal transfer characteristics of the system as a function of the spatial frequency. MTF is a good indicator of the spatial resolution of the image. The imaging setup and the edge test device used to implement the MTF is described by the IEC standard.[4,11,12] The test device for the determination of the MTF consists of a stainless steel plate (type 304) with dimensions of 0.8 mm thick, 120 mm long and 60 mm wide, covering half the irradiated field. The stainless steel is used as an edge test device. The edge was carefully polished straight.

The MTF tool for a mammography based CR system is different as compared to the general CR system. The impulse response is obtained from the sharp edged stainless steel plate tilted at about 2 degrees with respect to the lines or columns of the pixels and positioned along the central axis of the x-ray beam.

### 2.5 Noise power spectrum(NPS)

The NPS is a metric of image quality used to measure the noise characteristics and patterns in all frequencies of the image. The imaging setup used to implement the NPS was assessed according to the the IEC 62220-1-2 standard. The normalized NPS (NNPS) was used to compare the noise properties of different systems. The normalized noise power spectrum was calculated using uniform exposure images. The high-resolution phosphor imaging plate was placed directly upon the bucky table and exposed using the 2mm Al hardened beam.[3] NNPS is the NPS divided by the squared mean pixel value of the linearized image. The methods used to calculate the NPS using the uniform field images were similar to those used by Flynn.[13] The NPS is obtained by: (1) taking a flood exposure image at a preset dose, (2) sampling the image into smaller ROIs, (3) applying trend removal to

the linearized data, and finally, (4) calculating the 2D Fourier transforms of these regions and averaging them. We used the method described by Samie et al.[14] with the suggestions described by Park et al.[15] to implement this metric. The imaging setup used to implement the NPS is described by the IEC standard[16,17] description of these is beyond the scope of this text. The equation to obtain the NPS is shown below:

$$W_{out} = \frac{\Delta x \Delta y}{M \cdot 256 \cdot 256} \sum_{m=1}^{M} |\sum_{i=1}^{256}\sum_{j=1}^{256}(I(x_i, y_j) - S(x_i, y_j))exp(-2\Pi i(u_n x_i + v_k y_j))|^2, \quad (2)$$

where $\Delta$x $\Delta$y is the pixel spacing in respectively the horizontal and the vertical directions; M is the number of ROI's; I($x_i$,$y_j$) is the Linearize data; S($x_i$,$y_j$) is the optionally fitted two dimensional polynomial.

### 2.6 Detective quantum efficiency (DQE)

The DQE describes the efficiency of the detector of the system, and is used to compare the relative performance of different x-ray image detectors. This metric of image quality measures the transfer of signal to noise ratio from the input to the output of a detector. The ideal system DQE would start at unity and stay constant at unity to the highest frequency of interest. This metric is obtained by using the MTF and NPS. The MTF, NPS and DQE tools were evaluated on a standard iCRco's CR 3600 LF that was used as a test machine.

The greater the value of DQE, the more efficiently the detector records x-ray image information. The magnitude of DQE varies with effective beam energy, tending to fall as the beam energy increases. DQE is calculated from the MTF, NNPS and exposure to the system in terms of the mean number of x-ray photons incident per unit area using the expression:

$$DQE(f) = \frac{G \cdot MTF(f)^2}{q \cdot NPS(f)}, \quad (3)$$

where, G =Gain Factor, MTF(f)= presampled modulation transfer function NPS(f)= the noise power spectrum in mm2 measured at a given exposure & q is the square of ideal signal to noise ratio in mm2.[14] The variable 'q' in the equation is calculated as, $q = k_a \cdot SNR_{in}^2$, where, $K_a$= measured Air Kerma in Gy and $SNR_{in}^2$= the squared signal to noise ratio per Air Kerma[12] and is given by the IEC standard.

## 3. RESULTS AND DISCUSSION

### 3.1 Contrast Detail using the CDMAM Phantom

Four scans were acquired using 4 different values of Laser Power (mW) using an 80mW/658nm laser while the rest of the settings were kept constant. A Graphical User Interface (GUI) was developed for scoring the gold disks in the CDMAM phantom and the square blocks containing gold disks in the phantom were filled. A square block in the phantom filled with black color indicates that the gold disks can be seen while an empty block indicates that gold disks can't be seen. The pink line passing through the center is the gold standard for iCRco's CR3600 M based on the EUREF standards for CDMAM phantom. These objective measurements were obtained by 3 different readers who are responsible for performing Quality Control testing on CR systems.

### 3.2 Contrast to Noise Ratio (CNR)

The Contrast Plot and contrast to noise ratio(CNR) of step-wedge images at various Laser Powers (8mW-32mW) were obtained for comparison.

This test shows that contrast increases as we increase the laser power and reaffirms the results obtained from CDMAM phantom images. Using the CDMAM phantom, we observed more gold disks at a higher laser power. We also observed that the highest CNR was observed at 24 mW and the noise increased slightly as we went above 24 mW.

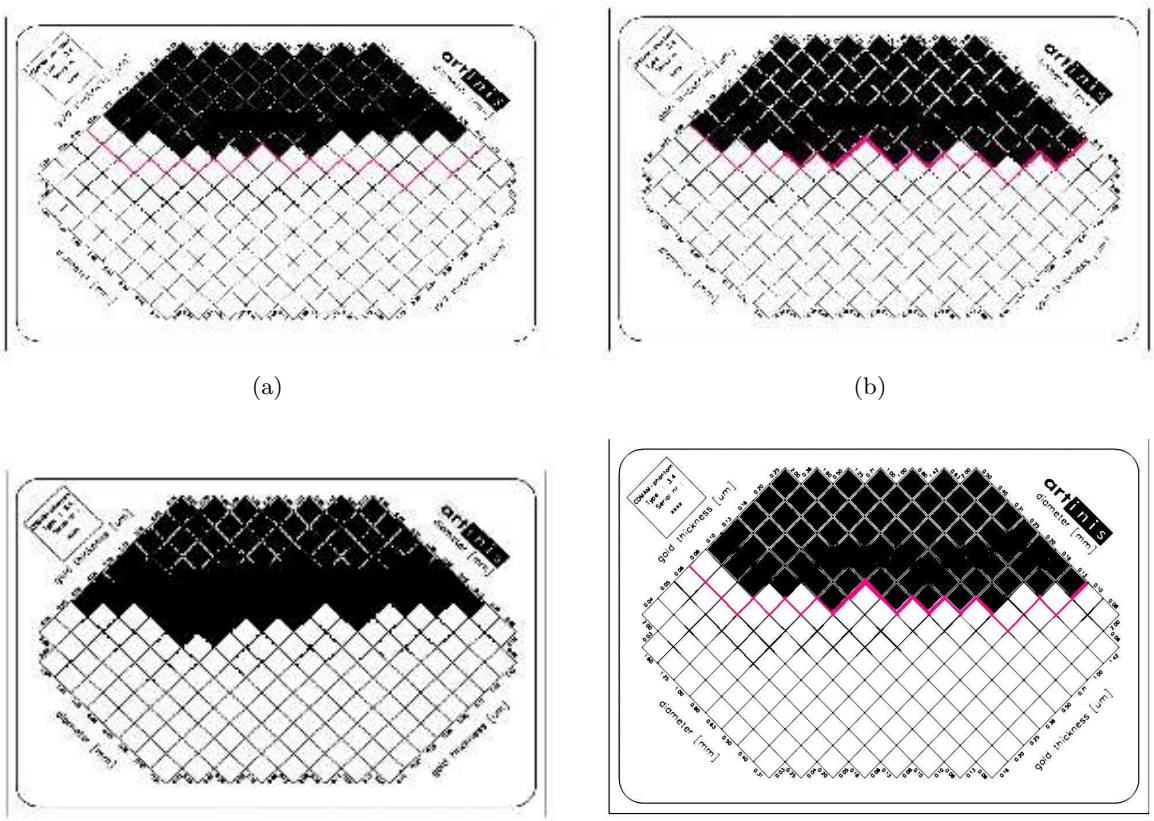

(a) (b)

(c) (d)

Figure 3. CDMAM phantom scores at different laser power voltages: (a) CDMAM Phantom results at Laser Power - 12 mW; (b) CDMAM Phantom results at Laser Power - 24 mW; (c) CDMAM Phantom results at Laser Power - 30 mW; and (d) CDMAM Phantom results at Laser Power - 36 mW

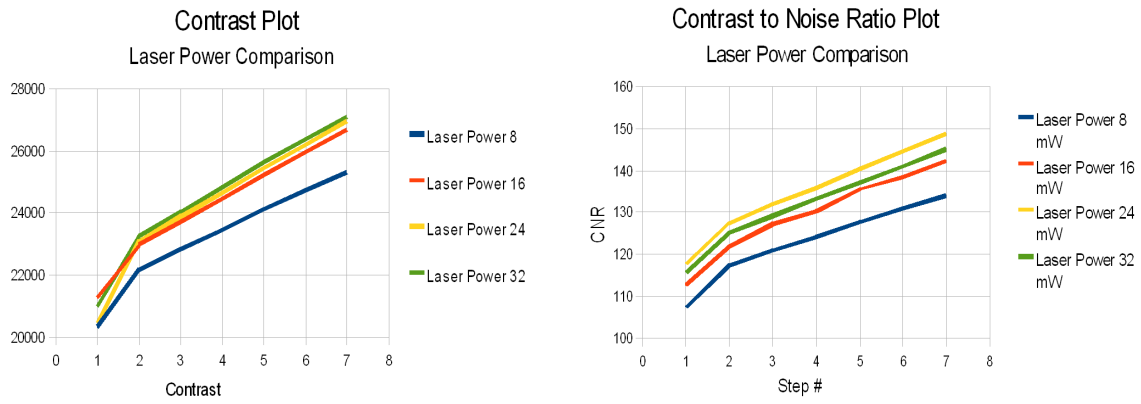


(a) (b)

Figure 4. (a) Absolute Contrast values varying with increasing Laser Power, (b) Contrast to Noise Ratio (CNR) varying with increasing Laser Power

### 3.3 MTF, NPS and DQE results

The MTF, NPS and DQE were used to determine the optimal PMT Voltage and Laser Power required to obtain better mammograms having improved spatial resolution and less noise. Figure 6(a) shows the MTF plot and we

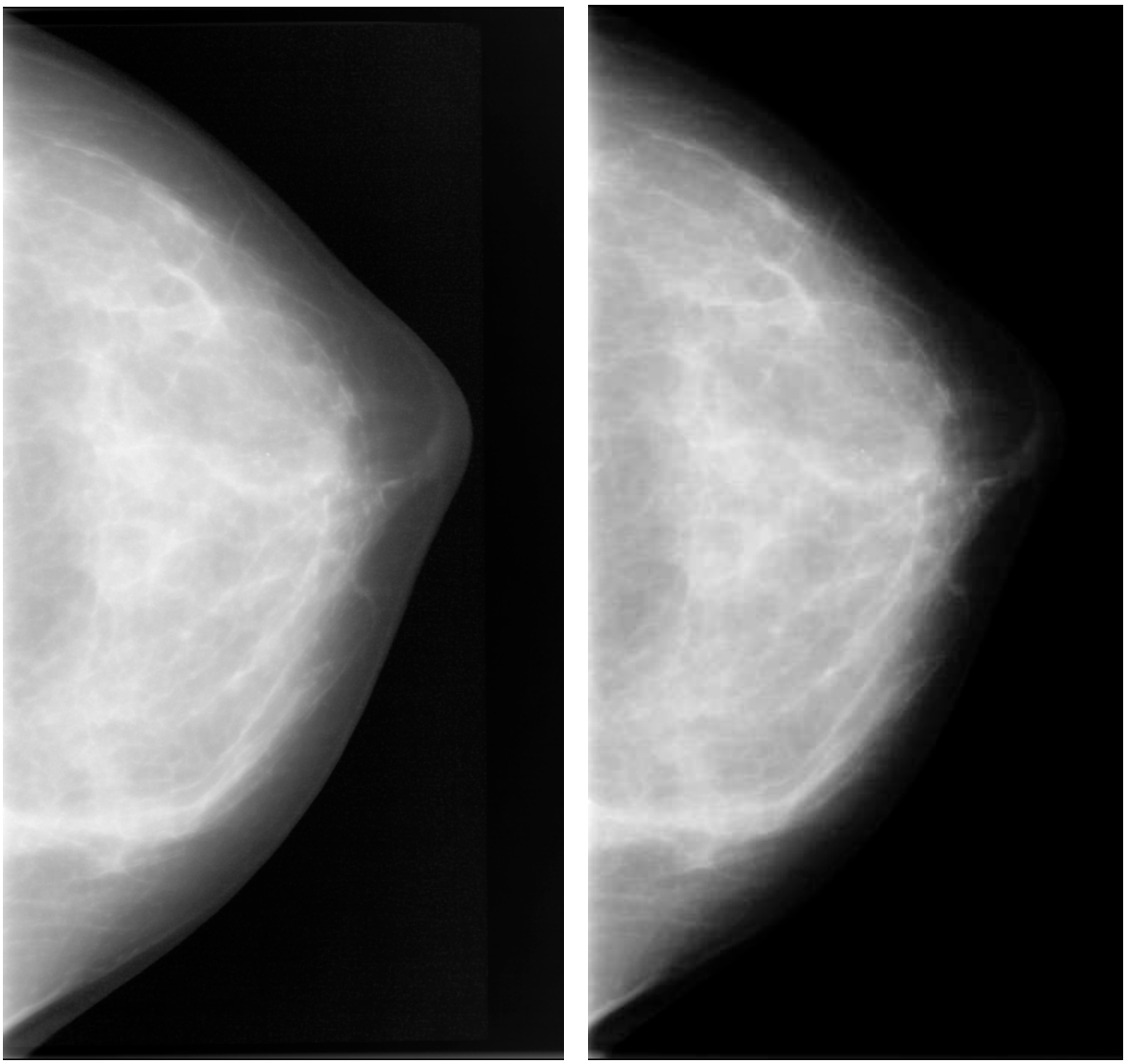

(a) (b)

Figure 5. (a) Anthropomorphic Phantom image at correct settings, (b) Anthropormorphic Phantom image at incorrect settings

can see that the spatial resolution is slightly lower when the laser power is lowered to 8mW. When the laser power is raised in intervals of 8 mW, the MTF quickly reaches a local maximum. Figure 6(b) shows the Normalized Noise Power Spectrum plot and we can see that the noise is higher in the system at lower laser power i.e. around 8-15 mW. When the laser power is raised higher, the noise levels lower down. Figure 6(c) shows the DQE plot for the iCRco's CR 3600 M as a function of spatial frequency. The value of the DQE obtained depends on the exposure.[18] The iCRco's CR system had a DQE of 28 % at laser power of 8mW while it increased slightly up to 32 % when the laser power was raised to 24mW. For DQE measurements, the Half-value layer (HVL) of the Mo anode and filter and 2 mm Al filtered beam was measured to be 0.56 mm. The decrease in DQE is continuous and very pronounced for the CR systems. This is caused due to the amount of structured noise and detective layer granularity.[18]

The Gammex 169 "Rachel" anthropomorphic breast phantom[19] was used for evaluation of effects of changing mammographic imaging parameters such as machine settings. Images of anthropomorphic breast (Rachel) phantom[19] were acquired using optimal and suboptimal settings for the PMT Voltage and Laser Power for the

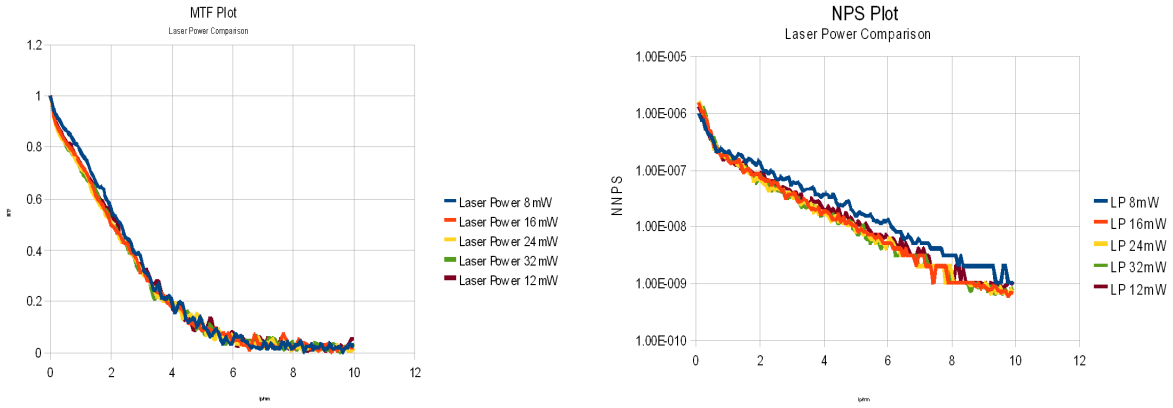


(a)




(b)

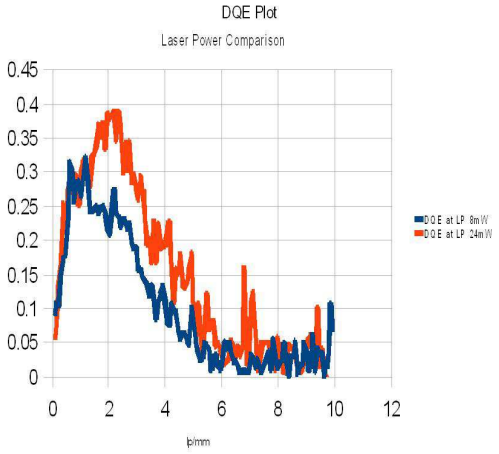


(c)

Figure 6. (a) Modulation Transfer Function (MTF) varying with increasing Laser Power, (b) Noise Power Spectrum (NPS) varying with increasing Laser Power, (c) Detective Quantum Efficiency (DQE) varying with increasing laser power

CR-3600M and the difference in contrast and noise was clearly visible between the two images. In the figure 5(a) the skin-line of the breast phantom is clearly visible and there is minor loss of spatial and contrast resolution in the image. In figure 5(b) the skin line can't be seen without adjusting the window/level.

Also, the storage phosphor detector and readout system have spatially dynamic nature and therefore pixel by pixel correction of phosphor nonuniformity is impractical. Kenneth et al.[3] have also reported that the CR images contain structured noise that originates at the storage phosphor, thus when the x-ray energy to the detector is increased, the noise component increases, resulting in decreased DQE with increased dose to the phosphor plate.[3] The measurements of MTF, NPS and DQE have been used a lot in comparing imaging systems from different companies but there has been very less written on trying to optimize the performance of an imaging system using the same tools. We have discussed how these tools can be used to optimize the performance of an imaging system by finding out the correct settings for the PMT voltage and laser power.

## 4. CONCLUSIONS

Metrics to characterize the imaging performance of CR based Mammography systems were described and practical software tools for optimizing the electro-optical components of the system were developed and validated. High-quality CR Mammography images were obtained by optimizing the contrast and spatial resolution of the system as measured by the available metrics, including the CNR, MTF, NPS, DQE and contrast-detail (CDMAM)

phantom. The tools used are an effective means of selecting optimal values for the electro-optical components of the system although there is a trade-off between contrast resolution, spatial resolution and detective quantum efficiency. The low DQE of the single-side read CR based mammography system can be attributed to the inherent x-ray absorption and light collection efficiency limitations of conventional single-side read CR systems.[18]

## ACKNOWLEDGMENTS

This work was supported by iCRco, Inc, Torrance, CA. The software programs to calculate the CNR and MTF are available for download as ImageJ plugins from the iCRco website at: http://www.icrcompany.com/physics.

## REFERENCES

[1] Young, K. C., Alsager, A., and Oduko, J. M., "Evaluation of software for reading images of the cdmam test object to assess digital mammography systems," *Medical Imaging 2008* **Proc. of SPIE Vol. 6913** (2008).

[2] Onishi, H., "Computed radiography - based mammography with 50 microns pixel size," *Acad Radiology* **16** (2009).

[3] Fetterly, K. A., "Performance evaluation of a "dual side read" dedicated mammography computed radiography systems," *Med. Phys. 30* **30 (7)** (2003).

[4] *Internation Standard IECCEI 62220-1-2, 2007-06.*

[5] Seibert, J. A., "Cassette-based digital mammography," *Technology in Cancer research and treatment* **3 (5)** (2004).

[6] Rowlands, J. A., "The physics of computed radiography," *Physics in medicine and biology* **47**, R123–R166 (2002).

[7] Karsemeijjer and Thijssen, "Determination of contrast-detail curves of mammography systems by automated image analysis in digital mammography," *Proceedings of the 3rd International Workshop on digital mammography* **32**, 155–160 (1996).

[8] *R. Visser and N. Karssemeijer "CDCOM Manual: software for automated readout of CDMAM 3.4 images".*

[9] Evans, D., "A comparison of the imaging properties of ccd based devices for small field digital mammography," *Phys. Med. Biol.* **47**, 117–135 (2002).

[10] Desai, N., Singh, A., and Valentino, D. J., "Practical evaluation of image quality in computed radiographic (cr) imaging systems," *Proceedings of SPIE* (2010).

[11] Carton, A.-K., "Validation of mtf measurement for digital mammography quality control," *Medical Physics 32* **32 (6)** (2005).

[12] Buhr, E., Gnther-Kohfahl, S., and Neitzel, U., "Simple method for modulation transfer function determination of digital imaging detectors from edge images," *Proceedings of SPIE* **5030**, 877–884 (2003).

[13] Flynn, M., "Experimental comparison of noise and resolution for 2k and 4k storage phosphor systems," *Med. Phys.* **26**, 1612–1623 (1999).

[14] Samei, E. and Flynn, M. J., "Physical measures of image quality in photostimulable phosphor radiographic systems," *SPIE* **3032**, 328–338 (1997).

[15] Park, H.-S., Cho, H.-M., Jung, J., and Lee, C.-L., "Comparison of the image noise power spectra for computed radiography," *Journal of Korean Physical Society* **54** (2009).

[16] "Medical electrical equipment characteristics of digital x-ray imaging devices part 1: Determination of the detective quantum efficiency," *International Electrotechnical Commission (IEC)* **IEC 62220-1** (2003).

[17] Illers, H., Buhr, E., Bergmann, D., and Hoeschen, C., "Measurement of the detective quantum efficiency (dqe) of digital x-ray imaging devices according to the standard iec 62220-1," *Proceedings of SPIE* **5368**, 177–187 (2004).

[18] Monnin, Gutierrez, and Bulling, "A comparison of the performance of digital mammography systems," *Med. Phys.* **34 (3)** (2007).

[19] Martin, C., "The importance of radiation quality for optimisation in radiology," *Biomedical Imaging and Intervention Journal* **3(2)** (2007).